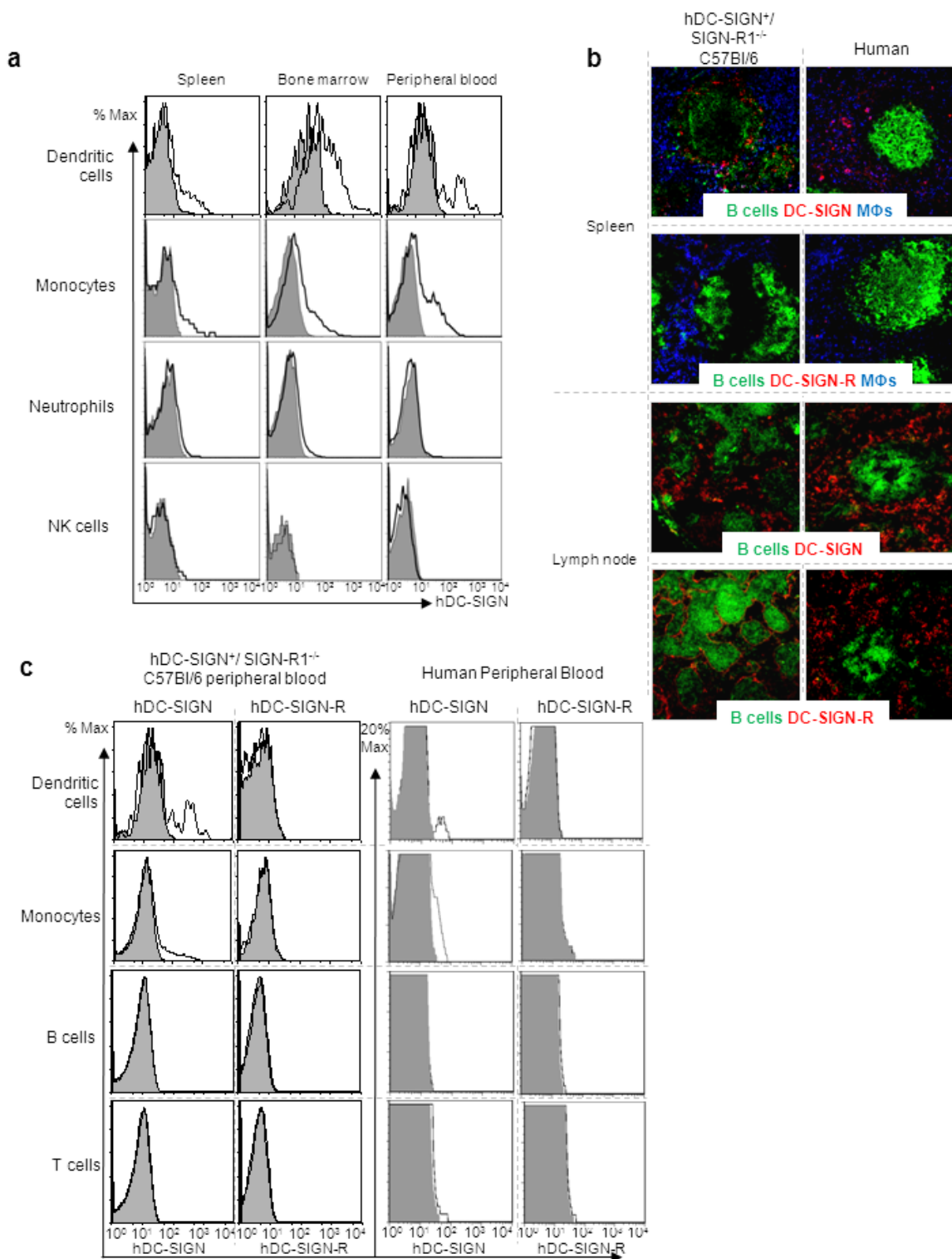


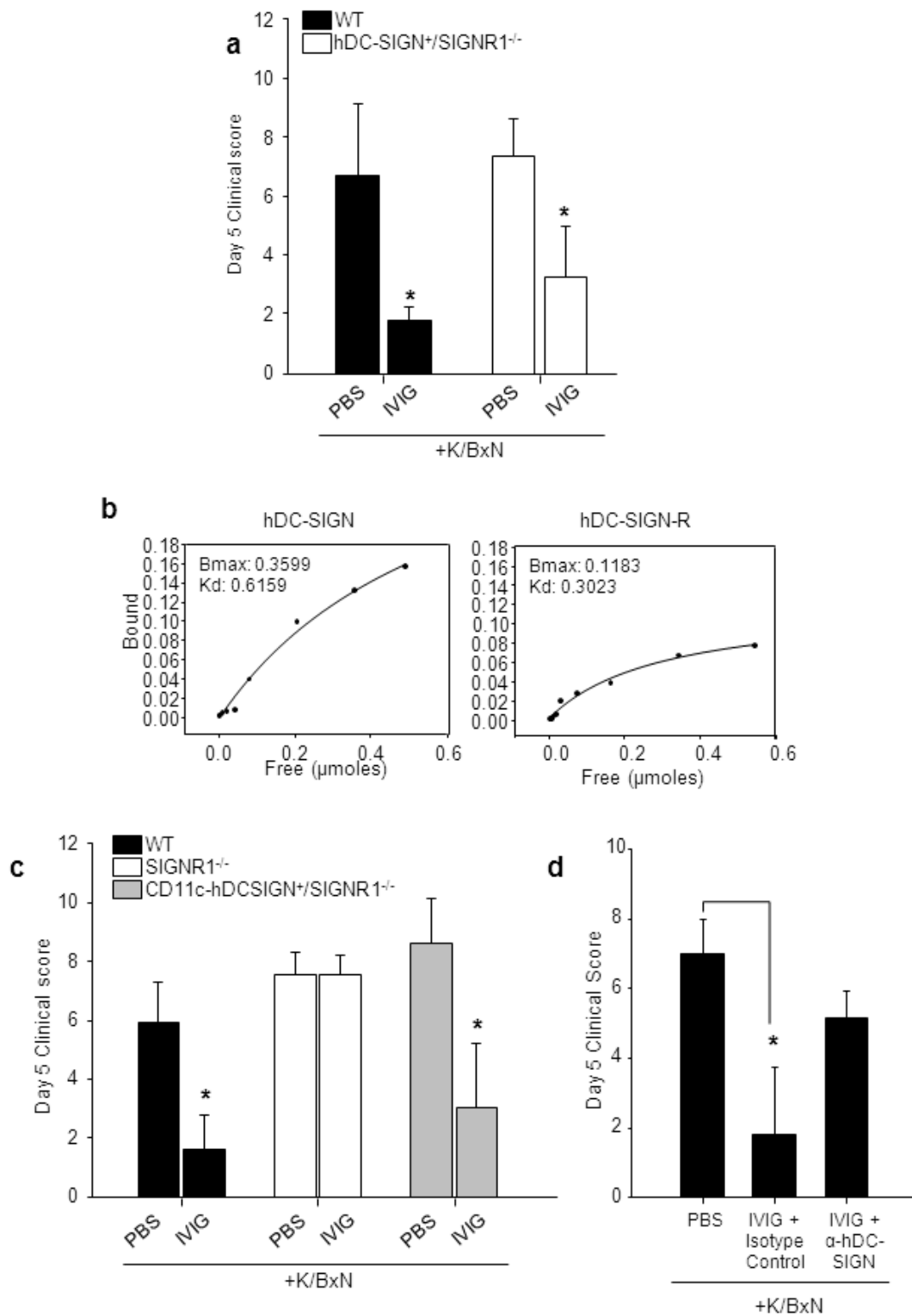
**Supplementary Figure 1. Anti-inflammatory activity of sFc.** a, Autoantibody immune complexes crosslink activating Fc receptors, promoting activation of macrophages, and

inflammation associated with autoantibody-mediated autoimmune disease. **b**, Following administration of IVIG, antibodies with sialylated IgG Fcs bind DC-SIGN<sup>+</sup> myeloid-derived cells promoting IL-33 expression, which activates FcεRI<sup>+</sup> innate leukocytes to produce IL-4. This cytokine promotes upregulation of FcγRIIB on macrophages, thereby increasing the activation threshold required to initiate inflammation.



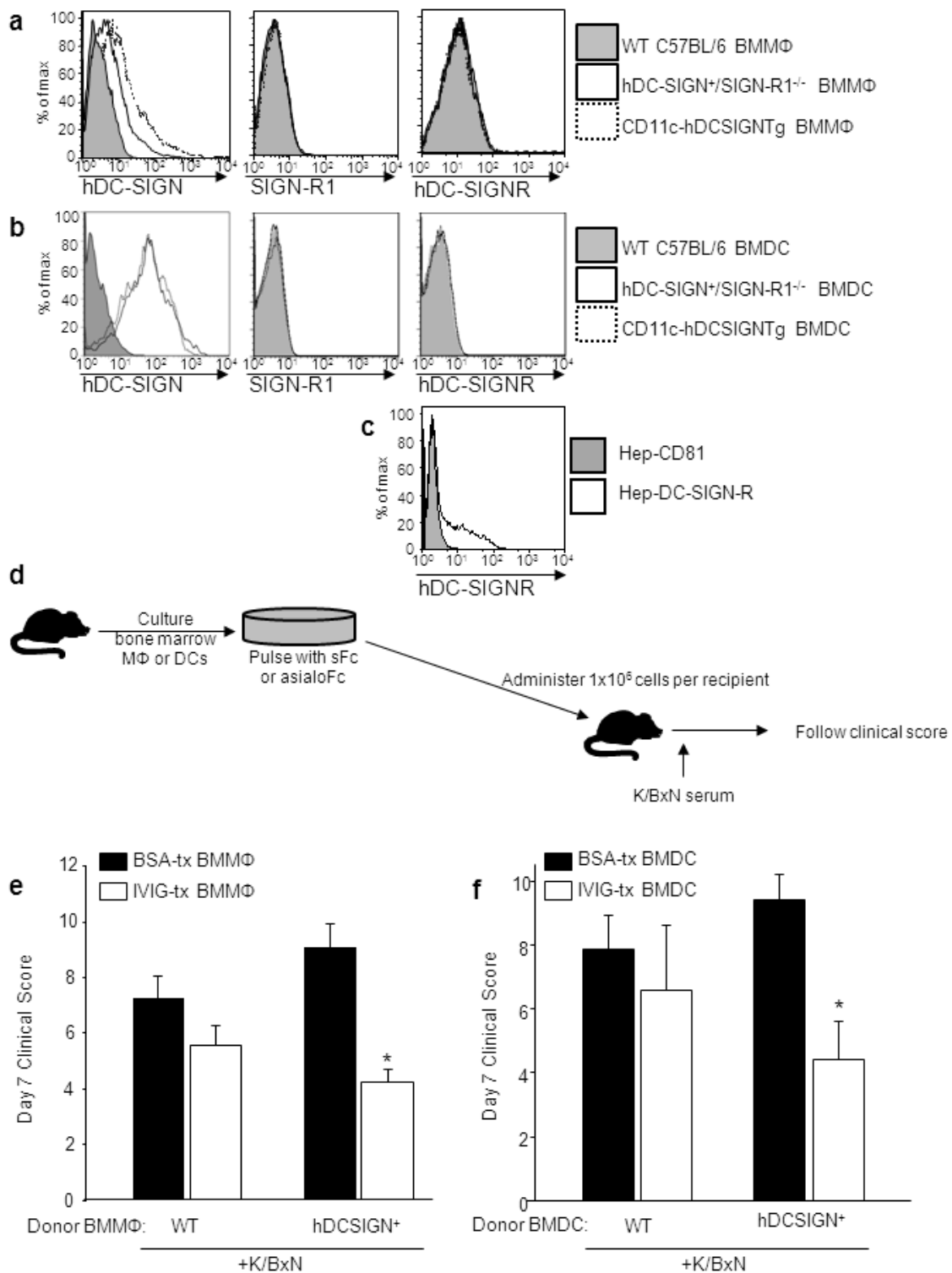
**Supplementary Figure 2. Characterization of hDC-SIGN<sup>+</sup> mice.** a, FACS analysis of hDC-SIGN expression on dendritic cells (CD11c<sup>+</sup> I-A<sup>b+</sup>), monocytes (CD11b<sup>+</sup> Ly6G<sup>-</sup>), neutrophils

(CD11b<sup>+</sup> Ly6G<sup>hi</sup>), and NK cells (CD19<sup>-</sup>, CD3ε<sup>-</sup>, NKp46<sup>+</sup>) recovered from spleen, bone marrow, and peripheral blood of hDC-SIGN<sup>+</sup>/SIGN-R1<sup>-/-</sup> (white histograms) and wild type (WT) control (gray histograms) mice. **b**, Expression patterns of hDC-SIGN and hDC-SIGN-R was compared between hDC-SIGN<sup>+</sup>/SIGN-R1<sup>-/-</sup> mouse and human lymphoid tissues. Spleen and lymph node cryosections were stained with α-hDC-SIGN or α-hDC-SIGN-R (red) in combination with B cell markers (green, α-B220 for mouse, α-CD20 for human) or macrophage markers (blue, α-F4/80 for mouse, α-CD68 for human) and visualized by fluorescence microscopy. **c**, hDC-SIGN and hDC-SIGN-R expression was compared on leukocytes recovered from hDC-SIGN<sup>+</sup>/SIGN-R1<sup>-/-</sup> mouse and human peripheral blood. Mouse leukocytes were stained for dendritic cells (CD11c<sup>+</sup> I-A<sup>b+</sup>), monocytes (CD11b<sup>+</sup> Ly6G<sup>-</sup>), B cells (CD19<sup>+</sup>), and T cells (CD3ε<sup>+</sup>), while human leukocytes were stained for dendritic cells (CD11c<sup>+</sup> HLA-DR<sup>+</sup>), monocytes (CD14<sup>+</sup> CD16<sup>dim</sup> CD19<sup>-</sup> CD3<sup>-</sup> CD56<sup>-</sup>), B cells (CD19<sup>+</sup>), and T cells (CD3<sup>+</sup>).



**Supplementary Figure 3. hDC-SIGN but not hDC-SIGN-R is required from IVIG anti-inflammatory activity.** **a**, WT (black bars) and hDC-SIGN<sup>+</sup>/SIGNR1<sup>-/-</sup> (white bars) were

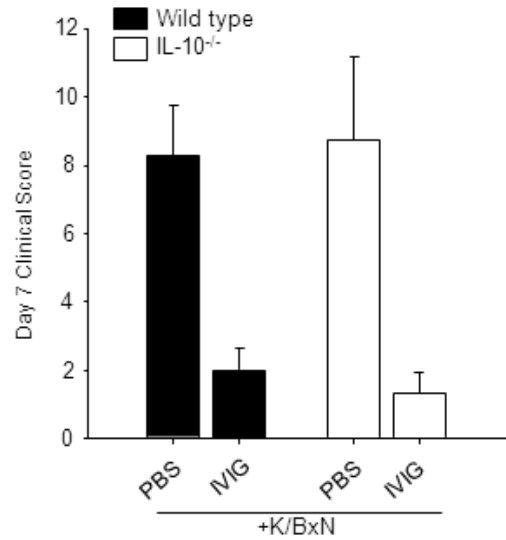
administered IVIG and K/BxN sera, and footpad swelling monitored over several days. Means and standard deviations of day 5 clinical scores are plotted. **b**, Saturation binding experiments were performed using cell lines that expressed hDC-SIGN or hDC-SIGN-R to determine their affinities for sFc (inset). **c**, Wild type (black bars), SIGN-R1<sup>-/-</sup> (white bars) and CD11c-hDC-SIGN<sup>+</sup>/SIGN-R1<sup>-/-</sup> (gray bars) mice were treated with K/BxN sera and IVIG, and footpad swelling monitored over several days. Means and standard deviations of day 5 clinical scores are plotted; \* $p < 0.01$  as determined by Tukey's posthoc test. **d**, hDC-SIGN<sup>+</sup>/SIGN-R1<sup>-/-</sup> BAC tg mice were administered K/BxN, IVIG, and 125ug of  $\alpha$ -hDC-SIGN or mouse IgG2a isotype control, and footpad swelling monitored. Day 5 clinical score means and standard deviations of 4 mice per group are plotted; \* $p < 0.05$  as determined by Tukey's posthoc test.



**Supplementary Figure 4. hDC-SIGN<sup>+</sup> cells transfer anti-inflammatory activity.** hDC-SIGN, SIGN-R1, and hDC-SIGN-R expression was compared on mature BMMΦ (a) and BMDC (b)

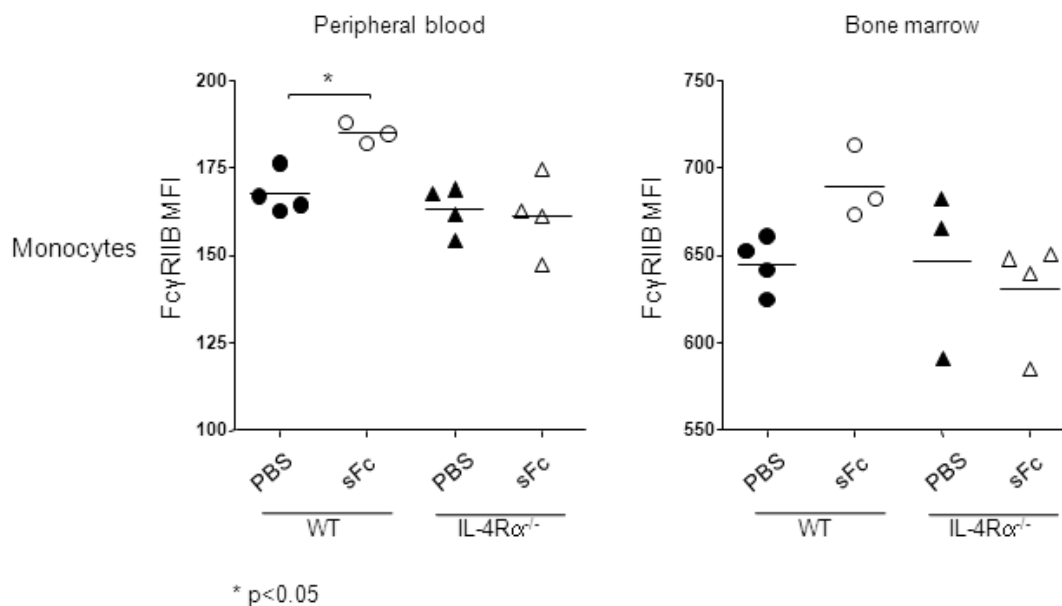
from wild type mice (gray fill), hDC-SIGN<sup>+</sup> mice (white fill), and CD11c-hDC-SIGN<sup>+</sup> mice (dotted line) by FACS. **c**, Hep-hDC-SIGN-R cells (white histograms) were stained for hDC-SIGN-R expression and compared to Hep-CD81 cells (gray histogram) to validate the  $\alpha$ -hDC-SIGN-R staining. **d**, A schematic representation for BM-derived cell transfer experiments is shown. Bone marrow progenitors were cultured into mature macrophages or dendritic cells. Differentiated cells were replated, pulsed with Fcs for 30 minutes, recovered and washed, and administered to mice that were then treated with K/BxN sera. BMM $\Phi$  (**e**) or BMDC (**f**) from WT and hDC-SIGN<sup>+</sup> mice were pulsed with BSA (15mg/ml, black bars) or IVIG (15mg/ml, white bars), and transferred to WT recipient mice which then received K/BxN sera. Footpad swelling was monitored over the next several days. Means and standard deviation of day 7 clinical scores are plotted; \* $p < 0.05$  as determined by Tukey's posthoc test.



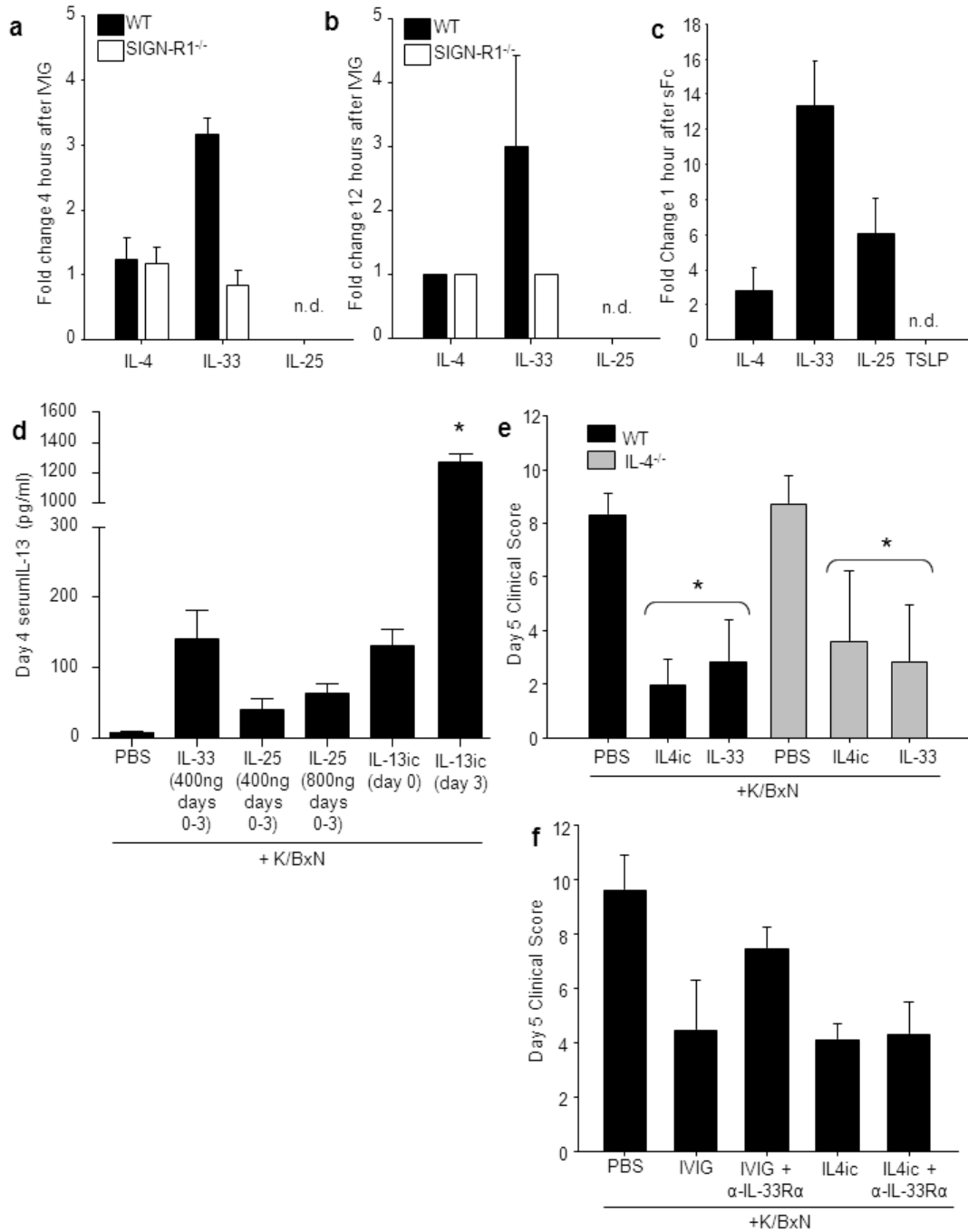


**Supplementary Figure 5. IL-10 is not required for the anti-inflammatory activity of IVIG.**

WT (black bars) and IL-10<sup>-/-</sup> mice (white bars) were administered K/BxN sera, some of which received IVIG, and footpad swelling monitored over the next several days. Means and standard deviations of day 7 clinical scores of 4-5 mice per group are plotted.

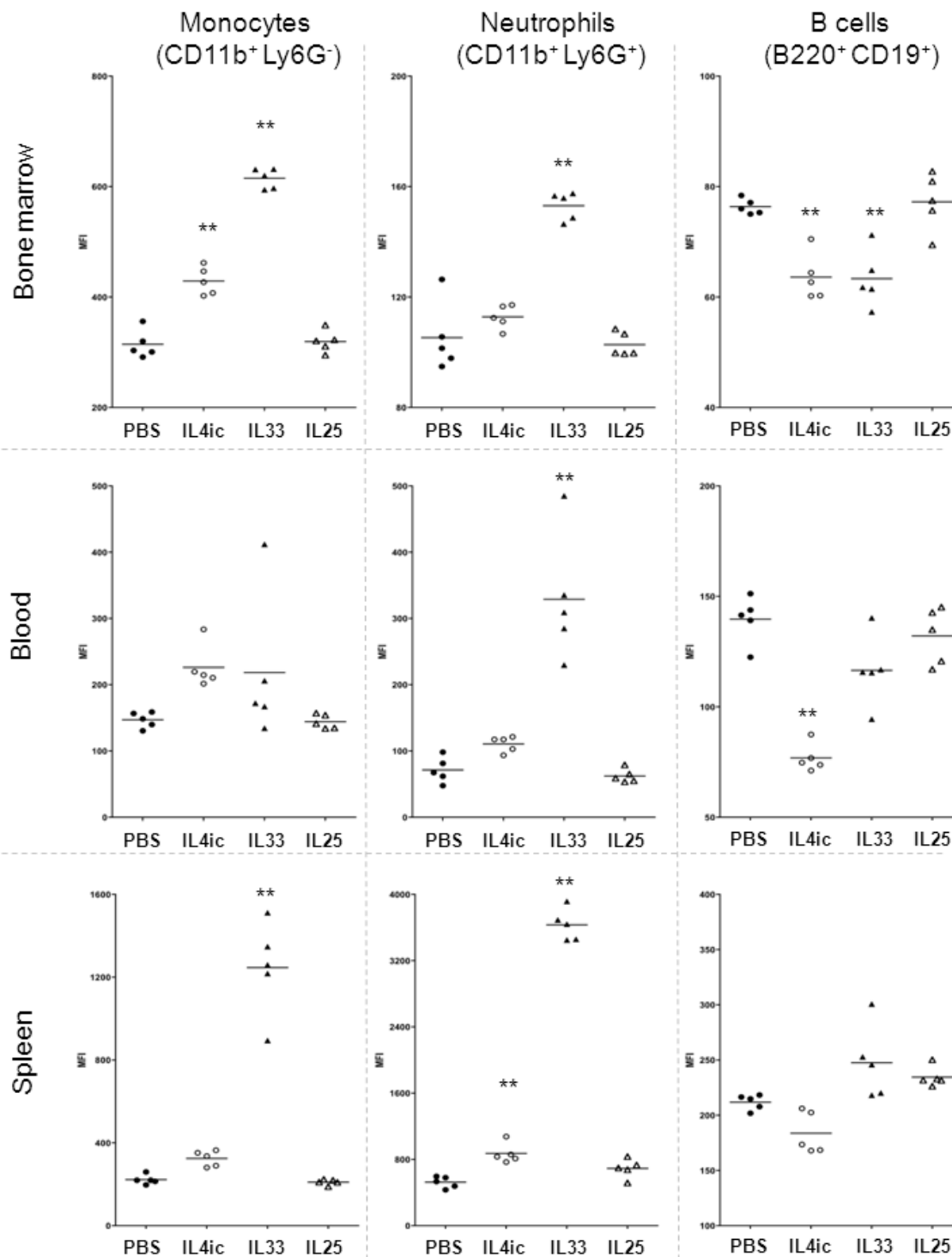


**Supplementary Figure 6. IL-4 receptor requirement for sFc triggered FcγRIIB upregulation.** WT or IL-4Rα<sup>-/-</sup> mice were administered PBS or sFc and one day later, surface expression of FcγRIIB on monocytes (CD11b<sup>+</sup> Gr1<sup>-</sup>) recovered from peripheral blood and bone marrow was determined by FACS. Mean fluorescence intensities (MFI) of 4 mice per group are plotted; \*p < 0.05 as determined by ANOVA followed by a Tukey's posthoc test.



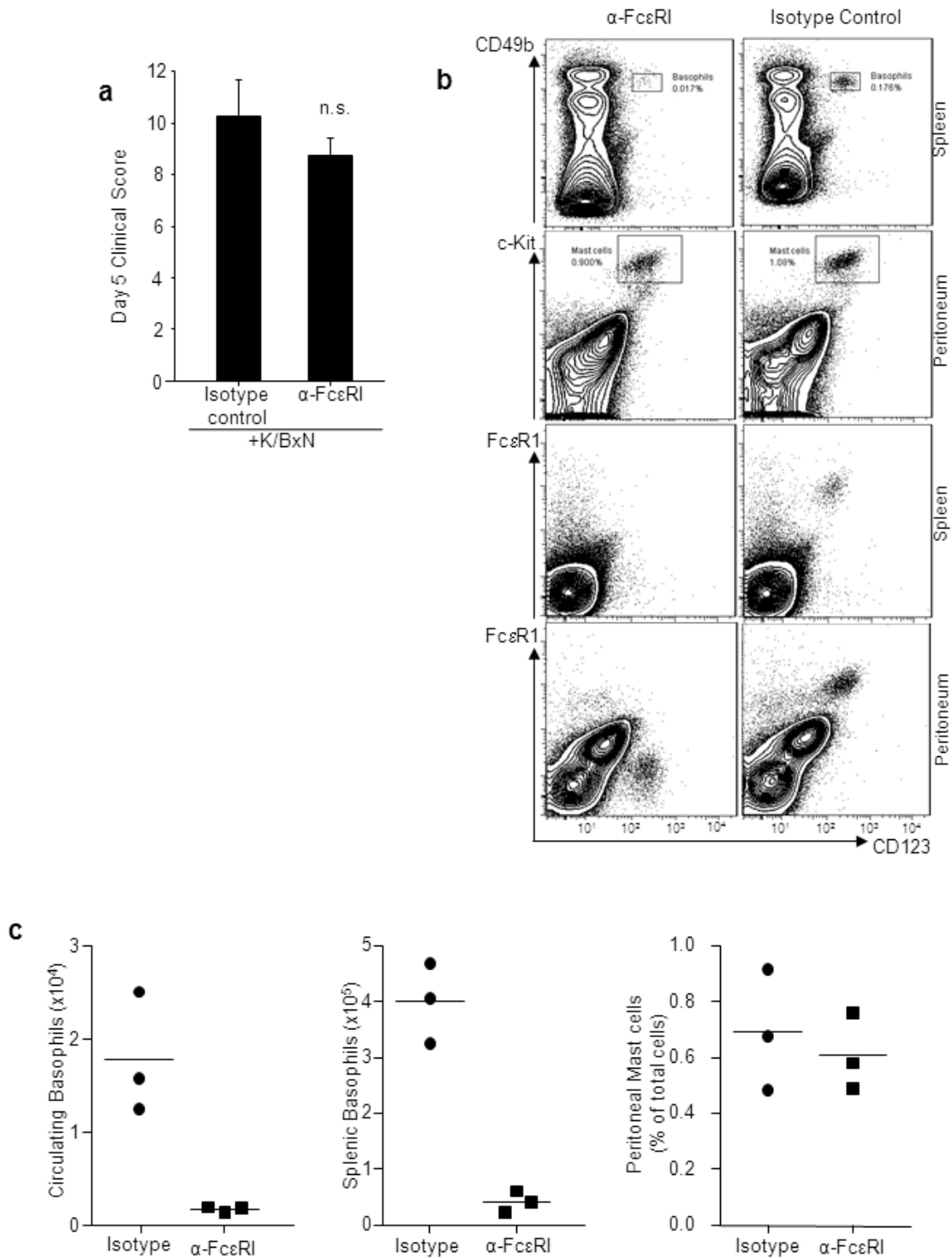
**Supplementary Figure 7. Analysis of IL-33 anti-inflammatory activity.** qPCR was performed on spleen samples were recovered from WT and SIGN-R1<sup>-/-</sup> mice administered IVIG 4 hours (**a**) and 12 hours (**b**) earlier. **c**, Spleens from sFc treated mice were recovered 1 hour after treatment, and qPCR was performed as described above. **d**, Mice were administered K/BxN along with

PBS, 400ng IL-33, 400ng IL-25, 800ng IL-25, biotinylated IL-13ic on day 0, or biotinylated IL-13ic on day 3. Also, on day 3, all mice (but IL-13ic treated groups) were administered 10 $\mu$ g of biotinylated  $\alpha$ -IL-13. All mice were bled the next day (day 4), and systemic IL-13 levels were determined. IL-25 is reported to induce expansion of IL-13 expressing populations<sup>16-18</sup>. Low systemic levels of IL-13 were detected in IL-25 and K/BxN treated mice, suggesting that IL-13 is sequestered or not released during inflammation, and thus unable to increase Fc $\gamma$ RIIB surface expression. **e**, WT (black bars) or IL-4<sup>-/-</sup> (gray bars) mice were administered PBS, IL-4ic, or IL-33 and K/BxN sera and monitored. The ability of exogenous IL-33 to protect IL-4<sup>-/-</sup> mice suggests the IL-13 induced by IL-33 (shown in **d**) is sufficient to increase Fc $\gamma$ RIIB surface expression and attenuate inflammation. Means and standard deviations of day 5 clinical scores from four mice are plotted. \* $p < 0.05$  as determined by ANOVA followed by a Tukey's posthoc test. **f**, K/BxN treated mice were administered IVIG or IL-4ic, some of which received  $\alpha$ -IL-33R $\alpha$ . Means and standard deviation of day 5 clinical scores are plotted.  $\alpha$ -IL-33R $\alpha$  treatment obscured IVIG protection of K/BxN inflammation, but did not affect IL-4ic protection, indicating IL-33 and the IL-33R $\alpha$  act downstream of IVIG, but upstream of IL-4 in this pathway.



**Supplementary Figure 8. Exogenous IL-4 and IL-33 upregulate monocyte surface expression of Fc $\gamma$ RIIB.** WT mice were administered PBS (black circles), IL-4ic (white circles),

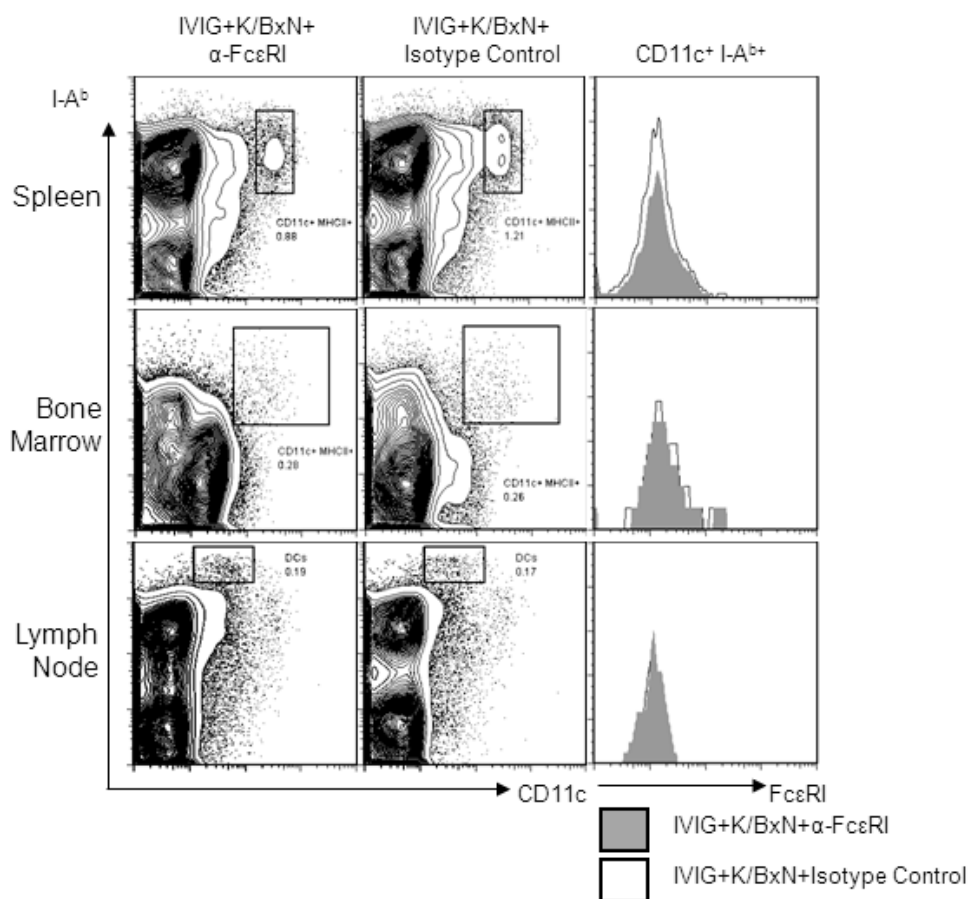
IL-33 (black triangles), or IL-25 (white triangles), and the next day, monocytes (CD11b<sup>+</sup> Ly6G<sup>-</sup>), neutrophils (CD11b<sup>+</sup> Ly6G<sup>+</sup>) and B cells (B220<sup>+</sup> CD19<sup>+</sup>) from bone marrow, spleen, and blood were subjected to FACS. Mean fluorescence intensities (MFI) of surface FcγRIIB staining of 5 mice per group are plotted; \*\*p<0.01 as determined by Tukey's posthoc test.



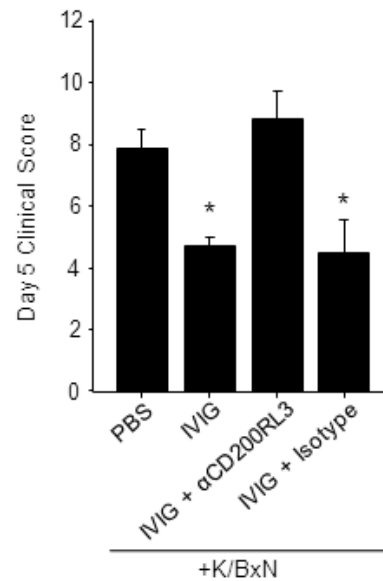
**Supplementary Figure 9. Selective depletion of basophils by  $\alpha$ -Fc $\epsilon$ RI treatment.** a, Wild type mice received K/BxN sera in conjunction with  $\alpha$ -Fc $\epsilon$ RI or isotype control antibodies, and

footpad swelling was monitored. Means and standard deviations of day 5 clinical scores are plotted; n.s. (not significant) as determined by Tukey's posthoc test. **b**, Basophil-depletion was evaluated in mice treated with  $\alpha$ -Fc $\epsilon$ RI or isotype control antibodies by FACS. Representative basophil (CD49b<sup>+</sup> CD123<sup>+</sup>) and mast cell (cKit<sup>+</sup> CD123<sup>+</sup>) percentages are inset, showing basophils but not mast cells are depleted following  $\alpha$ -Fc $\epsilon$ RI treatment. Fc $\epsilon$ RI staining is, however, blocked on peritoneal mast cells in  $\alpha$ -Fc $\epsilon$ RI treated but not isotype control treated mice. **c**, Basophil (CD49b<sup>+</sup> CD123<sup>+</sup>) and mast cell (c-Kit<sup>+</sup> CD123<sup>+</sup>) numbers in  $\alpha$ -Fc $\epsilon$ RI (black squares) or isotype control (black circles) treated mice were quantified by FACS are plotted.

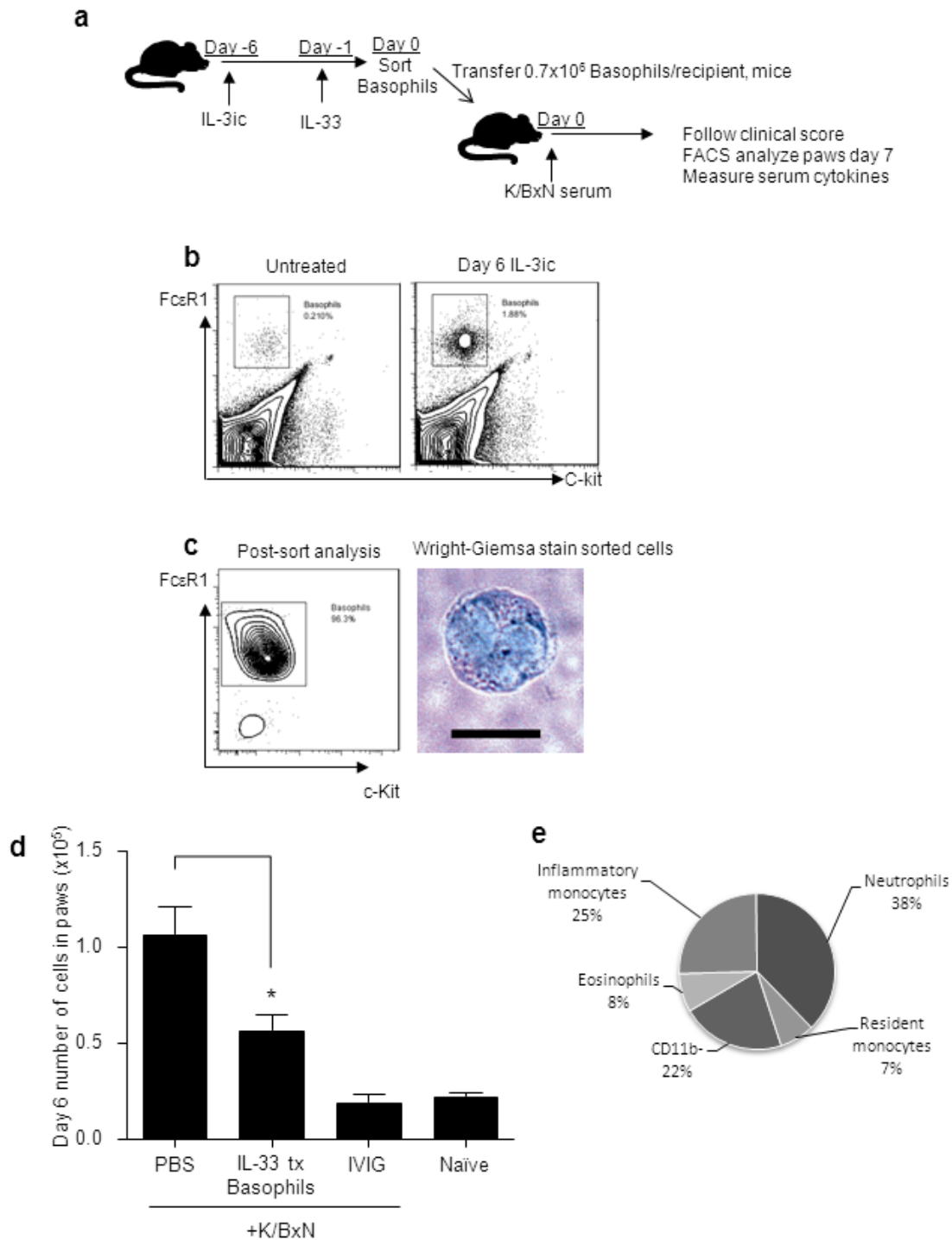




**Supplementary Figure 10. Dendritic cells are unaffected by  $\alpha$ -Fc $\epsilon$ RI treatment.** Dendritic cells have been reported to be affected by  $\alpha$ -Fc $\epsilon$ RI treatment<sup>19</sup>. Therefore, dendritic cells (CD11c<sup>+</sup> I-A<sup>b+</sup>) were analyzed in  $\alpha$ -Fc $\epsilon$ RI and isotype control treated mice, and histograms of gated dendritic cell populations expression of Fc $\epsilon$ RI is shown in the right column;  $\alpha$ -Fc $\epsilon$ RI treated (gray histograms), isotype control treated (white histograms).



**Supplementary Figure 11.  $\alpha$ -CD200RL3 treatment obscures IVIG anti-inflammatory activity.** Wild type mice were treated with K/BxN sera and IVIG (1g/kg). Some of the mice were treated with  $\alpha$ -CD200R3 antibody or rat IgG1 isotype control. Footpad swelling was monitored; mean and standard deviation of day 5 clinical scores of 5 mice per group are plotted; \* $p < 0.05$  as determined by Fisher LSD posthoc test.



**Supplementary Figure 12. IL-33 primed Basophils transfer anti-inflammatory activity.** **a**, A schematic of basophil transfer procedure is shown. Donor mice were treated with IL-3ic to expand basophils<sup>15</sup>. Five days later, the mice were administered PBS or IL-33. The next day (day

0), basophils (CD49b<sup>+</sup> FcεRI<sup>+</sup> c-Kit<sup>-</sup>) were FACS sorted, and administered to naïve recipient mice that then received K/BxN sera. **b**, Representative FACS plot showing basophil expansion (FcεRI<sup>+</sup> cKit<sup>-</sup>) by IL-3i.c. **c**, FACS sort purity of expanded basophils was assessed by FcεRI<sup>+</sup> DX5<sup>+</sup> cKit<sup>-</sup> cells, and cell morphology was characterized by staining sorted cells after cytopspin treatment using a Wright-Giemsa stain; scale bar 10um. **d**, The total number of leukocytes in the paws of mice treated with K/BxN sera and PBS, IL-33 treated FcγRIIB<sup>-/-</sup> basophils, or IVIG was compared to untreated (naïve) mice. Means and standard deviation of 4 mice per group are plotted. **e**, The relative percentages of leukocytes in K/BxN inflamed paws are plotted in a pie chart. The relative percentages were consistent and did not reflect differences in clinical score, however the total number of infiltrating cells (as shown in **d**) was reflective of clinical score.